# Experimental investigation of a 1 kA/cm$^2$ sheet beam plasma cathode electron gun

Niraj Kumar,[1,2,a)] Udit Narayan Pal,[1,2] Dharmendra Kumar Pal,[1] Rahul Prajesh,[1,2] and Ram Prakash[1,2]
[1]*CSIR-Central Electronics Engineering Research Institute (CSIR-CEERI), Pilani, Rajasthan 333031, India*
[2]*Academy of Scientific and Innovative Research (AcSIR), New Delhi, India*

(Received 26 November 2014; accepted 14 January 2015; published online 29 January 2015)

In this paper, a cold cathode based sheet-beam plasma cathode electron gun is reported with achieved sheet-beam current density ~1 kA/cm$^2$ from pseudospark based argon plasma for pulse length of ~200 ns in a single shot experiment. For the qualitative assessment of the sheet-beam, an arrangement of three isolated metallic-sheets is proposed. The actual shape and size of the sheet-electron-beam are obtained through a non-conventional method by proposing a dielectric charging technique and scanning electron microscope based imaging. As distinct from the earlier developed sheet beam sources, the generated sheet-beam has been propagated more than 190 mm distance in a drift space region maintaining sheet structure without assistance of any external magnetic field. © *2015 AIP Publishing LLC*. [http://dx.doi.org/10.1063/1.4906592]

## I. INTRODUCTION

The pseudospark discharge is a cold cathode discharge and is recognized as a class of discharge capable of producing round shaped electron beams with the highest combined current density and brightness than that of any other known type of electron sources.[1–4] However, such round shaped electron beams have their own limitations especially in high frequency microwave sources due to space charge effect.[5] The sheet-electron-beam has advantages in terms of reduced space charge field over round shaped beam[6] and can lead to effective conversion of its energy to RF. Also, the sheet-electron-beams have long generated impact in vacuum electronic devices.[7]

There are some researches for the sheet-electron-beam generation and its propagation with moderate beam current densities.[8,9] However, the transportation of the sheet-electron-beam in uniform axial magnetic field is still challenging in most microwave devices.[10,11] It is well-known that a sheet beam is not stable while propagating through a uniform magnetic field due to the ExB velocity shear effect. A diocotron instability results in beam kinks, vortices, and eventual filamentation,[11,12] which are the key indicators, and a uniform magnetic field may not be suitable to focus the sheet-beams. The diocotron instability is convective and it requires a finite length of propagation before becoming unacceptably pronounced.[13,14] The lower range for diocotron instability growth length is estimated as

$$L_d > v_z \frac{\omega_c}{\omega_p{}^2},$$

where $\omega_c$ represents the electron cyclotron frequency, $\omega_p$ represents the electron plasma frequency, and $v_z$ represents the electron velocity. In order to avoid diocotron instability, periodic focusing fields, such as periodic cusped magnetic fields and wiggler magnetic fields, have been studied.[12] Still such arrangements are complex and involve many fabrication difficulties.

This instability can also be suppressed by reducing the space charge effect during the sheet-beam propagation.[12] Such effects for cylindrical electron beam propagating in ion channel regime of beam generated plasma, where the space charge neutralization factor is greater than the critical neutralization factor, have been mostly studied.[15–17]

In this paper, we report first time a sheet-beam plasma cathode electron (SPCE)-gun based on pseudospark discharge for the generation of high current density sheet-electron-beam and its successful propagation without any assistance of external magnetic field, maintaining its sheet structure, inside the plasma filled drift space region. The developed gun consists of a trigger unit, a discharge unit, and hollow cathode-anode assemblies. The discharge in the gun is an axially symmetric self-sustained transient low pressure gas discharge. In the hollow cathode cavity, the plasma is a copious source of electrons, which has been used to generate the high current density sheet-electron-beam. Together with the delayed voltage breakdown and a fast current rise, we have achieved an intense sheet-electron-beam. The beam current density is diagnosed using three metallic isolated sheet arrangement whereas the beam size measurement is achieved by proposing a non-conventional dielectric charging and scanning electron microscope (SEM) based imaging technique.

## II. EXPERIMENTAL SETUP

### A. Vacuum system and SPCE-gun

The schematic view of the experimental setup for the developed SPCE-gun is shown in Fig. 1. The SPCE-gun consists of hollow cathode-anode geometries of typical sizes 60 mm diameter and 50 mm length. These hollow cavities

a)Author to whom correspondence should be addressed. Electronic mail: niraj.ceeri@gmail.com

 

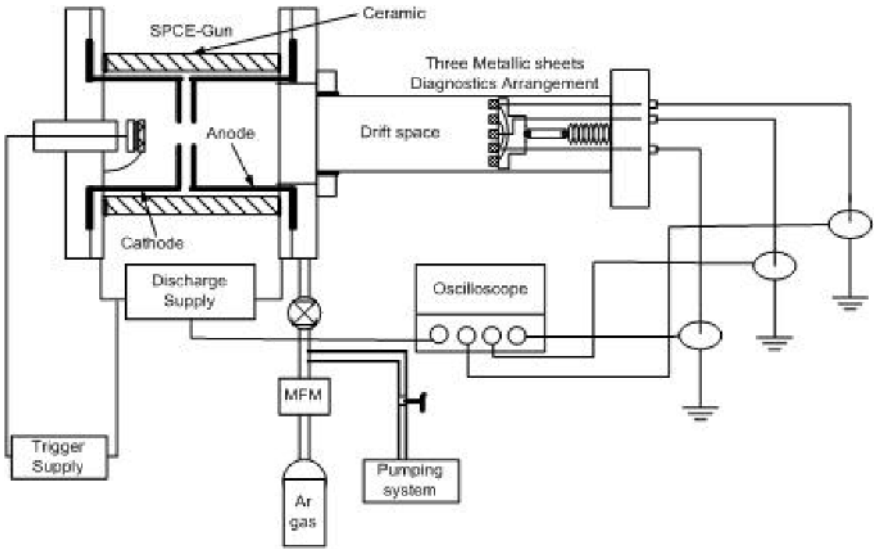


FIG. 1. The schematic view of the experimental setup.

have been isolated by ceramic disc in efficient manner to make arrangement leak tight. There are sheet form apertures in inverted cup structures with dimensions 7 mm × 1 mm of equal sizes on cathode and anode surfaces which are separated by 3 mm distance and facing each other. To provide seed-electrons inside the SPCE-gun, a trigger unit has been developed. In the trigger unit, a ferroelectric cathode has been used as an electron emission source. The used cathode in the trigger system works on the field emission based electron generation, and $\sim 10^9$-$10^{10}$ electrons are produced in ~300 ns time for the applied voltage of −1−−3 kV. The amount of the seed-electrons is controlled by varying the applied potential.

The hollow anode assembly has been connected with the drift space region for the sheet-beam characterization which is a circular glass tube (see Fig. 1). Before creating plasma discharge, the developed SPCE-gun along with the drift tube assembly has been evacuated up to base pressure $\sim 10^{-6}$ Torr with the help of turbo molecular pump (Pfeiffer Model TC 400) and rotary pump (Pfeiffer Model Duo 5M). The chamber is flushed couple of times with argon gas in controlled manner with the help of mass flow meter through connecting gas lines. The chamber has been evacuated again up to the base pressure and has been monitored by the pressure gauge (Pfeiffer Model D-35614). The argon gas pressure has been maintained below the self-breakdown condition required for this gas at fixed inter-electrode gap against an applied voltage. With the appropriate discharge power supply (up to −25 kV), connected in series with 1 MΩ resistor and in parallel with 200 nF capacitor, the plasma discharge has been produced inside the hollow cathode using seed-electrons generated by the trigger source. The discharge in the SPCE-gun has been studied for various ranges of applied voltages and corresponding operating pressures. These are typically between 5-20 kV and 250-65 mTorr, respectively.

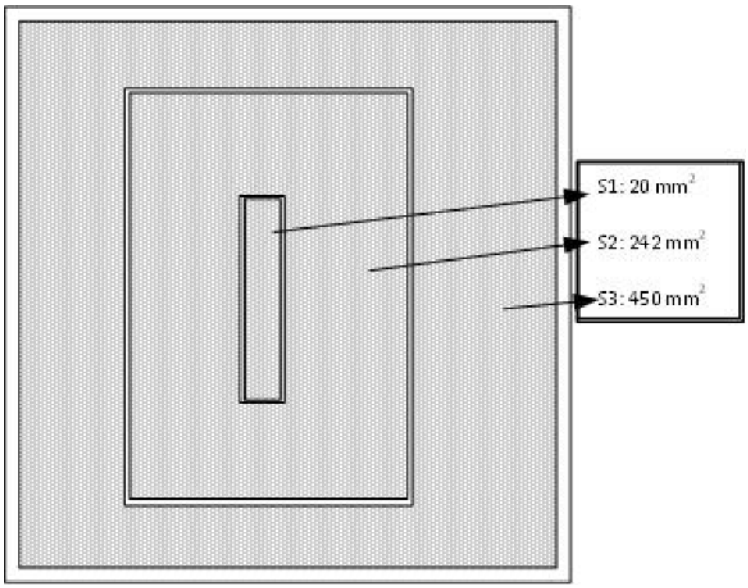


FIG. 2. Schematic view of the three metallic-sheets.

### B. Sheet-beam diagnostic methods

The generated sheet-electron-beam has been propagated inside the drift space region where it has been detected and characterized using two different diagnostic methods. In the first method, a simple technique has been developed as focusing and defocusing point estimations inside the drift space region. The technique comprises of three aligned rectangular stainless steel metallic-sheets (S1, S2, and S3 with corresponding areas 20 $mm^2$, 242 $mm^2$, and 450 $mm^2$, respectively) (see Fig. 2), which are mounted on Teflon base and are connected to the axial motion feedthrough. These sheets are facing anode aperture and are separated by 0.25 mm for their isolation. The rectangular metallic sheets are connected with insulated ports and wires passing through three calibrated current transformers (CTs) (Model 110, Pearson Current Monitor). The currents corresponding to the sheet-electron-beam, collected by the three rectangular sheets, have been measured using oscilloscope (Tektronix DPO 4054).

Another diagnostic technique based on dielectric charging and the SEM based imaging has been developed. The technique is able to provide the exact shape and size estimations of the sheet-electron-beam. In this technique, a dielectric surface of 1 $\mu$m $SiO_2$ layer is grown thermally on a rectangular sample of silicon substrate (28 mm × 20 mm), which has been mounted separately on a Teflon base and connected to the axial motion feedthrough inside the drift space region (see Fig. 1). The substrate is facing always anode aperture. The samples before and after the sheet-electron bombardment have been analyzed using SEM based imaging technique (JEOL, JSM 6390LV).

## III. RESULTS AND DISCUSSION

A typical V-I characteristic of the developed SPCE-gun at applied voltage 20 kV and working argon pressure 10 Pa is shown in Fig. 3. This figure also shows dI/dV curve that has been obtained from the V-I characteristic and clearly depicts two distinct phases of the electron beam currents occurring at two different times during the discharge. In the hollow cathode phase, the obtained beam current is ~35 A with beam energy ~15 keV whereas in conducting phase, these are ~483 A and ~3.9 keV, respectively.

These current phases are part of the plasma discharge. In fact, the applied potential between the hollow cathode-anode geometries increases due to the presence of energetic seed-electrons and the working pressure that has been kept below the self-breakdown potential. These seed-electrons lead to the collisions and ionization with the gas atom, and this process results into the formation of plasma inside the hollow cathode. During the hollow cathode discharge, the electrons get trapped in the large dynamic sheath fields inside the hollow cavity and make oscillations.[18] The electrons lose their maximum energy in ionization and excitations and finally diffuse through the aperture during the hollow cathode phase.[19] The electron density increases during the hollow cathode phase which later forms the conductive phase of the beam.

The energetic component of the sheet-electron-beam is formed during the hollow-cathode phase whereas the low energy beam component is formed when the applied voltages get collapsed due to conductive channel formation between the hollow cathode-anode and are responsible for these distinct phases observation in the beam generation (see Fig. 3).

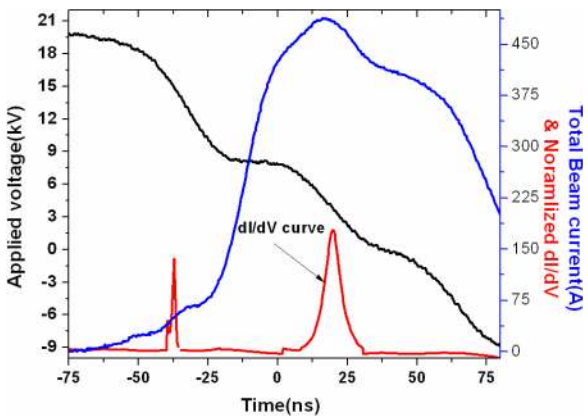


FIG. 3. V-I characteristics of the developed SPCE-gun at 20 kV applied voltage and Ar gas pressure 10 Pa. The total beam current profile is the sum of currents collected by all the three metallic-sheets S1, S2, and S3.

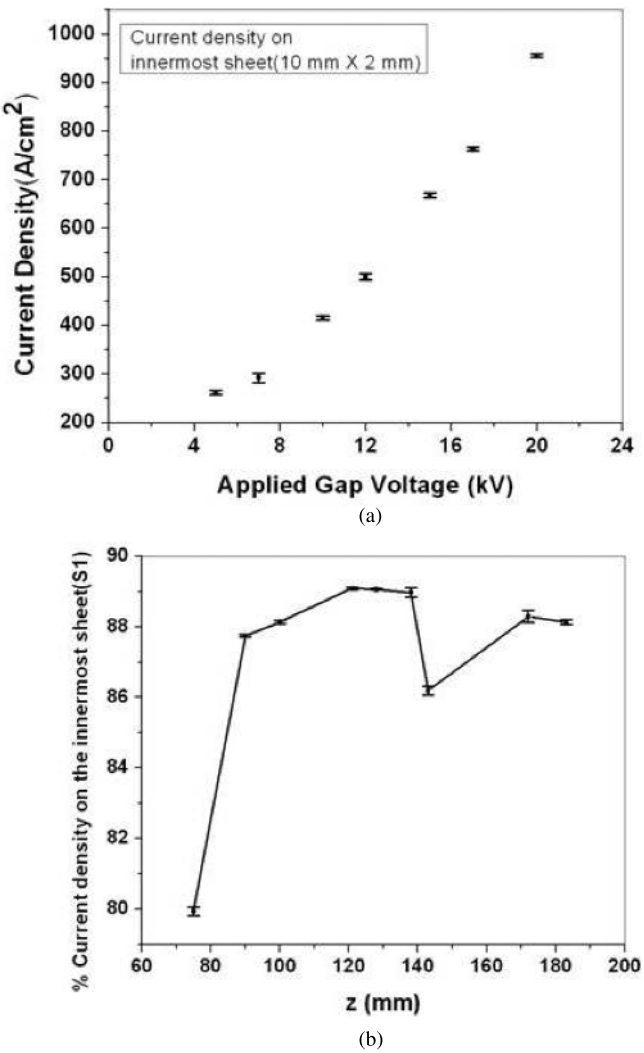


FIG. 4. Sheet beam analysis on the innermost sheet (S1: 20 $mm^2$); (a) current density for z = 190 mm at different applied gap voltages and (b) percentage current density for applied voltage 17 kV at different drift space locations.

For the efficient sheet-beam generation from the developed source, the trigger position β (i.e., distance between cathode aperture and trigger surface) has also been optimized at different non-self-breakdown pressures of argon gas by keeping the other parameters constant. The optimized β is found to be 8 mm and 10 mm for the applied voltages 17 kV and 20 kV, respectively. For the estimation of the focusing and defocusing points of the beam, the beam current density has been estimated on the innermost sheet S1 (20 $mm^2$) at the optimized trigger positions. Fig. 4(a) shows the beam current density at z = 190 mm (i.e., the distance from the cathode aperture) and at different applied gap voltages in the drift space region whereas Fig. 4(b) shows the percentage current density on the innermost collector sheet with respect to the total sheet-beam current density at different locations keeping applied gap voltage ~17 kV.

Figure 4(a) clearly shows the increasing trend of the beam current density with the increase in the applied voltage. As the applied voltage increases, the discharge current increases,[16] which subsequently results in to the higher beam current density at higher applied voltages. This is due to the fact that at the higher applied voltages, the positive accelerating field penetrates to the larger extent and creates more and more ionization. This figure further illustrates that the sheet-electron-beam current density ~1 $kA/cm^2$ has been achieved from this developed SPCE-gun for its maximum applied gap voltage ~20 kV (see Fig. 4(a)). The percentage current density variation on the innermost sheet, as shown in Fig. 4(b), clearly gives the sheet-beam focusing points inside the drift space region. This figure also says that more than 80% of the total beam current density is concentrated on the inner most sheet S1 and also depicts that at z = 120 mm the beam is more focused than that z = 73 mm. This has helped in identifying the focusing and defocusing locations inside the drift space region. Since there is no external applied magnetic field, this observation further confirms the space-charge neutralization effect when the sheet-electron-beam travels in the ion channel regime on the beam envelop leading to focus the sheet-beam.

The bombardment of the electron-beam on the dielectric surface (i.e., $SiO_2$) leads to accumulate the beam electrons. The SEM based images have confirmed the electron-beam in the sheet form. The SEM images of such samples are shown in Figs. 5(a) and 5(b) for fixed applied voltage at two different locations whereas Figs. 6(a) and 6(b) show such images for two different applied voltages at fixed location. These sheet-beam images also clearly depict the deviations in the size of the beam relative to the originating aperture size (7 mm × 1 mm). The found maximum deviation in the sheet-beam is ~22% along the

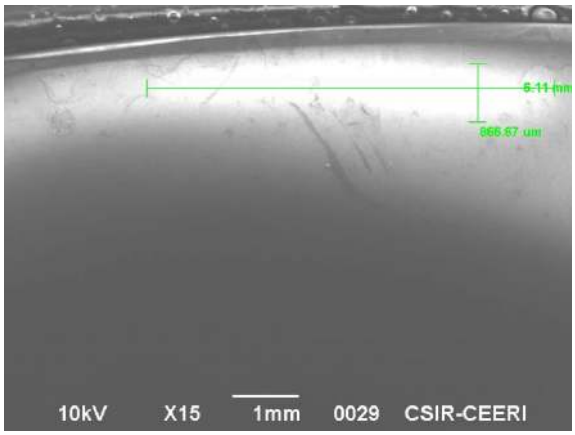


(a)

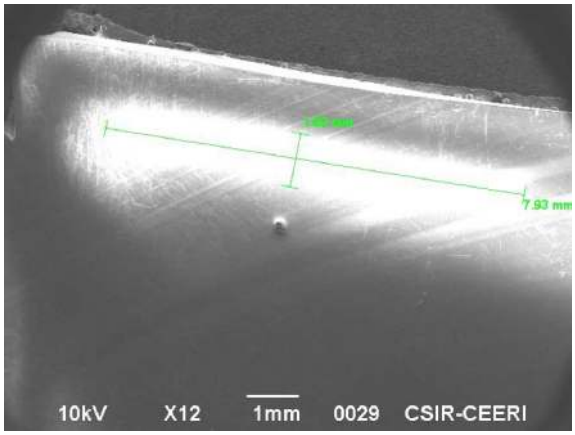


(b)

FIG. 5. SEM image of dielectric collector (a) at z = 90 mm, 17 kV (beam size 6.11 mm × 0.866 mm) and (b) at z = 143 mm, 17 kV (beam size 7.93 mm × 1.02 mm).

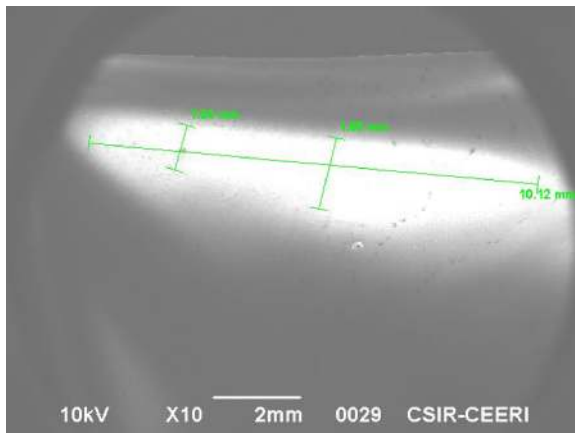


(a)

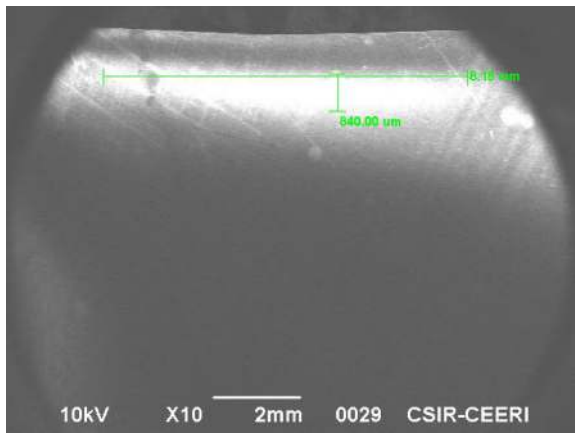


(b)

FIG. 6. SEM image of dielectric collector (a) at z = 190 mm, 10 kV (beam size 10.12 mm × 1.65 mm) and (b) at z = 190 mm, 20 kV (beam size 8.18 mm × 0.84 mm).

longer side and along the shorter side it is ~19% while propagating 190 mm distance inside the drift space region. These results have also been utilized for the comparative analysis of the beam size under same operating conditions as explained in Figs. 4(a) and 4(b).

The images shown in Figs. 5(a) and 5(b) confirm that the percentage current density on the innermost sheet at the fixed applied voltage 17 kV is more at z = 90 mm than that of z = 143 mm (i.e., due to reduced beam area), and the same has been clearly depicted in Fig. 4(b). Moreover, Figs. 6(a) and 6(b) confirm the similar behavior of the beam compression (i.e., again due to reduced beam area) with respect to higher applied voltages as shown in Fig. 4(a). Consequently, a good agreement between two diagnostic methods has been achieved.

## IV. CONCLUSIONS

A sheet-electron-beam with current density ~1 kA/cm$^2$ has been successfully generated by developing a trigger based SPCE-gun. The sheet-beam has been propagated more than 190 mm in the drift space region without any assistance of external magnetic field inside the hollow cathode region of the gun. The sheet-beam has been analyzed using three metallic sheet arrangement, and the same has been correlated with the dielectric charging technique. A good agreement is obtained between two analyses. The maximum deviation obtained from the SEM imaging in the sheet-beam is ~22% along the longer side while along the shorter side it is ~19% during its 190 mm propagation inside the drift space region.

## ACKNOWLEDGMENTS

The authors gratefully acknowledge Dr. Chandra Shekhar, Director, CSIR-CEERI for his kind support and Mr. Prem Kumar, CSIR-CEERI for his technical help in SEM based imaging. The authors also like to thank CSIR for the financial assistance for this work under CSIR Network Project No. PSC0101.

[1]The Physics Applications of Pseudosparks, NATO ASI Series B, edited by M. A. Gundersen and G. Schaefer (Plenum, New York, 1990), Vol. 219.
[2]K. Frank and J. Christiansen, IEEE Trans. Plasma Sci. **17**, 748 (1989).
[3]A. W. Cross, H. Yin, W. He, K. Ronald, A. D. R. Phelps, and L. C. Pitchford, J. Phys. D: Appl. Phys. **40**, 1953 (2007).
[4]H. Yin, A. W. Cross, W. He, A. D. R. Phelps, K. Ronald, D. Bowes, and C. W. Robertson, Phys. Plasmas **16**, 063105 (2009).
[5]P. A. Sturrock, J. Electron. Control **7**, 162 (1959).
[6]A. Gokhale, P. Vyas, J. Panikar, Y. Choyal, and K. P. Maheshwari, Pramana **58**, 67 (2002).
[7]J. X. Qiu, B. Levush, J. Pasour, A. Katz, C. M. Armstrong, D. R. Whaley, J. Tucek, K. Kreischer, and D. Gallagher, IEEE Microwave Mag. **10**, 38 (2009).
[8]B. D. McVey, M. A. Basten, J. H. Booske, J. Joe, and J. E. Scharer, IEEE Trans. Microwave Theory Tech. **42**, 995 (1994).
[9]X. Zhang, V. L. Granatstein, W. W. Destler, S. W. Bidwell, J. Rodgers, S. Cheng, T. M. Antonsen, B. Levush, and D. J. Radack, IEEE Trans. Plasma Sci. **21**, 760 (1993).
[10]J. Booske and M. Basten, IEEE Trans. Plasma Sci. **27**, 134 (1999).
[11]K. T. Nguyen, J. A. Pasour, T. M. Antonsen, P. B. Larsen, J. J. Petillo, and B. Levush, IEEE Trans. Electron Devices **56**, 744 (2009).
[12]J. H. Booske, B. D. McVey, and T. M. Antonsen, J. Appl. Phys. **73**, 4140 (1993).
[13]H. C. Chen, IEEE Trans. Nucl. Sci. **32**, 2380 (1985).
[14]R. C. Davidson, H. W. Chan, C. Chan, and S. Lund, Rev. Mod. Phys. **63**, 341 (1991).
[15]D. M. Goebel, Phys. Plasmas **6**, 2225 (1999).
[16]N. Kumar, U. N. Pal, D. K. Verma, J. Prajapati, M. Kumar, B. L. Meena, M. S. Tyagi, and V. Srivastava, J. Infrared, Millimeter, Terahertz Waves **32**, 1415 (2011).
[17]S. K. Karkari, S. Mukherjee, and P. I. John, Rev. Sci. Instrum. **71**, 93 (2000).
[18]A. Anders, S. Anders, and M. A. Gundersen, Phys. Rev. Lett. **71**, 364 (1993).
[19]L. C. Pitchford, J. Appl. Phys. **75**, 7227 (1994).